

Linkage of Late-Onset Fuchs Corneal Dystrophy to a Novel Locus at 13pTel-13q12.13

Olof H. Sundin,^{1,2} Albert S. Jun,¹ Karl W. Broman,³ Sammy H. Liu,¹ Siobhan E. Sheehan,¹ Elizabeth C. L. Vito,¹ Walter J. Stark,¹ and John D. Gottsch¹

PURPOSE. To identify the gene locus underlying the inheritance of late-onset Fuchs corneal dystrophy (FCD) in a large white kindred.

METHODS. Genotypes of small tandem repeat polymorphisms were obtained from 17 affected and 3 unaffected family members, followed by genetic linkage analysis.

RESULTS. In this family, classic late-onset FCD appeared to be inherited as a single, dominant Mendelian trait. In two exceptional sibships, however, children aged 10 and 13 years had FCD. In each sibship, both parents were found to be affected, opening the possibility that this unusually early age of onset was the result of homozygosity for an FCD mutation. Genotype results, however, were not consistent with consanguinity of the parents, who appear to have independent cases of FCD. A whole-genome linkage scan mapped FCD to a single locus at 13pTel-13q12.13, with significant two-point LOD scores of 3.91 at *DI3S1236* and 3.80 at *DI3S1304*. The 26.4-Mb disease interval contains the chromosome 13 nucleolus organizer (*RNR1*), the centromere, and 44 annotated protein-encoding genes. So far, exons of 10 of these genes have been screened, but no mutations have been found.

CONCLUSIONS. *FCD1* is the first genetic locus to be identified for late-onset FCD, a common disease of the aging cornea. The exceptional early onset of the disease observed in two children is unusual and might be the result of digenic interaction between *FCD1* and an independent late-onset FCD mutation. (*Invest Ophthalmol Vis Sci.* 2006;47:140-145) DOI:10.1167/iov.05-0578

Fuchs corneal dystrophy (FCD) is a degenerative disorder specific to the corneal endothelium¹⁻⁴ which affects roughly 4% of the population more than 40 years of age.⁵ It is distinguished from other corneal disorders by the progressive formation of guttae, which are microscopic refractile excrescences of Descemet's membrane, a collagen-rich basal lamina secreted by the corneal endothelium.^{6,7} From onset, it often takes two decades for FCD to impair endothelial cell function

seriously,^{5,8} leading to stromal edema and impaired vision.^{9,10} Currently, the only effective means of restoring vision in advanced cases is penetrating keratoplasty; FCD is one of the most common indications for this type of transplantation surgery.¹¹

Although Fuchs first described this disease in the early 20th century, its pathogenesis remains poorly understood. With regard to its genetics, large families exhibiting autosomal dominant inheritance of FCD have long been reported in the literature.¹²⁻¹⁴ The first progress toward identifying loci and gene mutations associated with familial FCD has been provided by a rare subtype of FCD characterized by atypical histopathology and disease onset in early childhood.¹⁴ This rare condition is caused by point mutations in the *COL8A2* gene,^{8,15} which encodes the $\alpha 2$ subtype of collagen VIII, a major component of Descemet's membrane. Although *COL8A2* disease has provided important evidence that implicates Descemet's membrane as the site of primary defects that cause FCD, we still have no convincing evidence that *COL8A2* mutations are involved in the more common late-onset form of this disease.^{8,16}

For late-onset familial FCD, the existence of additional gender-related genetic or physiological factors are suggested by the consistent observation of a ~2.5:1 ratio of affected females to males.^{5,8} This ratio is not explained by the greater frequency of women in older populations, or by simple autosomal dominant inheritance of the disease. Even though a combination of genetic, gender-related and environmental factors are thought to underlie most common diseases, large families with apparent dominant inheritance of FCD are surprisingly prevalent. On closer examination, as many as 50% of clinical patients with FCD have siblings, parents, or offspring who are also affected.^{5,8} In this study, we mapped the first genetic locus for late-onset FCD. In one large family it followed Mendelian inheritance as a single autosomal dominant trait.

METHODS

Patients

Family members for this study were recruited, examined and DNA samples obtained through procedures approved by the Institutional Review Board for Human Subjects Research at the Johns Hopkins University School of Medicine, according to the Declaration of Helsinki. Written consent was provided by each study participant, or by one of their parents.

Determination of Phenotype, Disease Severity, and Corneal Photography

Individuals were examined and photographed to document guttae by slit lamp biomicroscopy. A confocal specular microscope¹⁷ (ConfoScan3; Nidek Technologies, Vigonza, Italy) was used to view the guttae. Grading followed the scale proposed by Krachmer et al.,⁵ with Grade 0 indicating no disease, as defined by fewer than 11 central guttae. In this study, none of the unaffected cases had more than two central guttae. Grade 1, which represented definitive onset of the disease, was indicated by 12 or more central, nonconfluent guttae in at least one eye. Grade 2 patients exhibited a zone of confluent central guttae 1 to 2 mm in horizontal width,

From the ¹Center for Corneal Genetics, Cornea and External Disease Service, and the ²Laboratory of Developmental Genetics, The Wilmer Eye Institute, The Johns Hopkins University School of Medicine, Baltimore, Maryland; and the ³Department of Biostatistics, The Johns Hopkins Bloomberg School of Public Health, Baltimore, Maryland.

Supported by The Faller Family LLC and National Eye Institute Grant R01 EY013610 (OHS).

Submitted for publication May 11, 2005; revised July 10 and August 17, 2005; accepted November 29, 2005.

Disclosure: O.H. Sundin, None; A.S. Jun, None; K.W. Broman, None; S.H. Liu, None; S.E. Sheehan, None; E.C.L. Vito, None; W.J. Stark, None; J.D. Gottsch, None

The publication costs of this article were defrayed in part by page charge payment. This article must therefore be marked "advertisement" in accordance with 18 U.S.C. §1734 solely to indicate this fact.

Corresponding author: John D. Gottsch, 321 Maumenee Building, The Wilmer Eye Institute, Johns Hopkins Hospital, 600 N. Wolfe Street, Baltimore, MD 21287; jgottsch@jhmi.edu.

whereas in grade 3, this area of confluence had expanded to 2 to 5 mm, and in grade 4 its width was greater than 5 mm. Grade 5 was the same as grade 4, but also exhibited edema of the corneal stroma and/or epithelium.

Genotyping and Linkage Analysis

Blood (~10 mL) was collected and frozen at -20°C. DNA was extracted (Qiagen, Santa Clara, CA), and genotyped for 399 polymorphic linkage markers, using the MD10 set of fluorescent primers (Applied Biosystems, Inc. [ABI], Foster City, CA) using an automated DNA sequencer (Prism 377; ABI). Data processing and genotype assignment were performed on computer (GeneScan 3.1 and Genotyper 2.1, respectively; ABI). RelCheck confirmed pedigree relationships, and Pedcheck¹⁸ identified Mendelian inconsistencies. Two-point linkage was performed using MLINK.¹⁹ SimWalk2 version 2.89²⁰ was used for multipoint linkage and haplotype analysis. Unaffected individuals under 50 years of age were excluded from the analysis because of the late-onset nature of the disease. Marker allele frequencies were estimated by counting alleles of all genotyped members of the pedigree. Genetic markers and linkage distances were from the Marshfield maps,²¹ and map positions were from the physical genome map.

Screening Gene Exons for Mutations

Coding exons and their flanking splice-sites, the most common sites for disease-causing mutations,²² were PCR amplified from genomic DNA with custom primer pairs, purified and then sequenced with an automated sequencer (model 3730; ABI). Trace chromatogram data were viewed on computer (Sequencher 3.0 software) and manually screened for heterozygous sequence variants. Experimentally determined nucleotide sequences were compared with published sequences by alignment and coassembly, using the software. Genes already screened and their cDNA accession numbers are CRYL1 NM_015974; GJA3 NM_021954; GJB2 NM_004004; GJB6 NM_006783; FGF9 NM_002010; LOC387911 NM_001007537; MGC48915 NM_178540; MRP63 NM_024026; SGCG NM_000231; and TUBA2 NM_006001.

RESULTS

The Family and Its Clinical Phenotypes

A four-generation white pedigree with 20 affected individuals was assembled after discussions with an initial proband (Fig. 1, arrow). FCD was diagnosed using slit lamp biomicroscopy and assigned to severity grades (see Methods and Fig. 1). The distribution of individuals confirmed or presumed affected was generally consistent with Mendelian inheritance of a single dominant locus. In addition to apparent transmission from parent to child, the ratio of affected to unaffected individuals approximated a 1:1 ratio in the full pedigree. The excess of patients with FCD in the linkage pedigree (see Fig. 4) is an artifact of preferentially selecting those affected, who tend to be more informative because of the late onset of the disease.

The presence of late-onset disease in this family was established by two criteria. First, in all cases that were studied in detail and assigned a grade of severity, the clinical appearance of the posterior cornea by slit lamp and specular microscopy revealed lesions indistinguishable from those of common late-onset FCD. At early to intermediate stages, this was characterized by large, individual guttae with a distinctive peaked appearance.^{8,17} Second, the age-severity profile of this family was found to be generally consistent with that of late-onset FCD, which typically takes about two decades to progress from onset to end-stage disease.^{5,8} Those affected in generation II, who ranged from 74 to 84 years, all showed advanced FCD at grades 3 or 4, whereas in generation III, affected siblings of

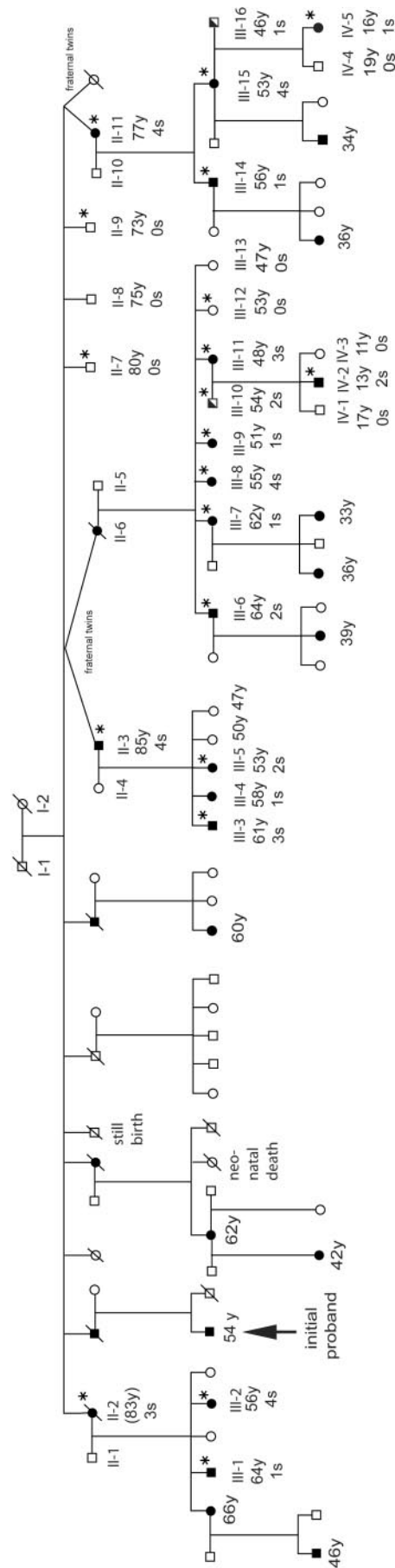


FIGURE 1. Dominant inheritance of Fuchs' corneal dystrophy. This pedigree presents all members of the first three generations of the AM kindred. *Arrow*: initial proband; *squares*: males; *circles*: females; *filled symbols*: FCD; *open symbols*: unaffected or not known to be affected; *diagonal slashes*: deceased. Members of the subpedigree used to calculate genetic linkage are identified by a Roman numeral indicating generation, followed by an Arabic numeral. *Asterisk*: those who contributed genotype data to the linkage analysis. Age in years is indicated below each individual for whom affection status was known with reasonable confidence. A severity grade is indicated for affected and unaffected individuals examined in detail. Two unrelated males who married into the family have symbols with a *diagonal black-and-white* sector to indicate that their FCD is not due to shared ancestry with the founders (I-1 and I-2) of this kindred.

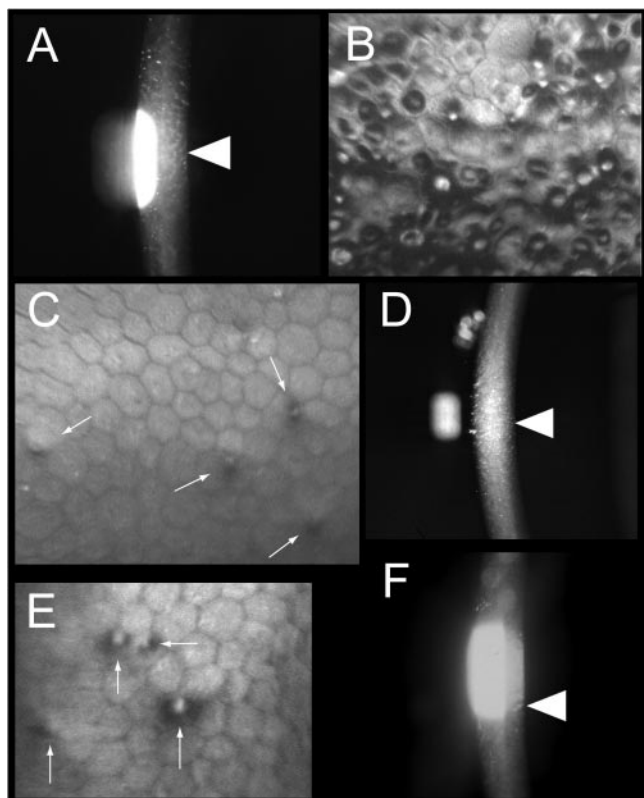


FIGURE 2. Clinical features of parents and children with FCD. Slit-lamp biomicroscopy photographs and/or confocal microscopy images of affected individuals. Since both eyes showed similar disease, only one from each patient is shown. Corneal guttae are indicated to the left of white arrowheads (A, D, F). (A, B) Mother (III-12) demonstrating moderate to severe corneal guttae. (C) Father (III-11) demonstrating scattered corneal guttae. (D, E) Child (IV-2) with moderate corneal guttae. (F) Child (IV-5) with early-stage FCD.

ages 45 to 64 were typically at grades 1 and 2, with only a few at grades 3 and 4 (Fig. 1).

Exceptional Cases of Early-Onset of Disease

Two affected women of generation III had husbands who were also affected with FCD (Fig. 1, III-10, III-16). Of special interest was the unusual diagnosis of FCD in two of their children. In one family, a 10-year-old boy (IV-2) was affected with grade 2 disease, whereas in the other family, a 13-year-old girl (IV-5) had grade 1 FCD. Although at first we suspected distant consanguinity of the parents, family members maintained that the two husbands were completely unrelated, a statement that was later supported by haplotype analysis of the genotype data.

With regard to clinical features of these families, the mother of the 10-year-old boy exhibited extensive corneal guttae when viewed by slit lamp microscopy, as indicated by white arrows in Figure 2A. Specular microscopy of the same eye (Fig. 2B) demonstrated moderate to severe cornea guttae. Specular microscopy of the father, who had grade-1 FCD, revealed scattered corneal guttae of conventional appearance (Fig. 2C). Slit lamp examination of the 10-year-old boy (Fig. 2D), revealed many scattered, individual central guttae, and specular microscopy (Fig. 2E) established that these were of conventional FCD morphology. Examination of the 13-year-old girl from the other sibship indicated a slightly earlier stage of the disease (Fig. 2F). Although the ages of these two patients classified them as having early-onset FCD, the clinical appearance of the guttae was indistinguishable from those of classic late-onset FCD, and

did not have the unusual, fine-grained appearance that we and others have characterized in patients with FCD with *COL8A2* mutations.^{8,15}

Initial Genetic Linkage

To map the disease trait, DNA isolated from individuals marked by asterisks in Figure 1 was genotyped for 399 polymorphic markers on all autosomes. Because of the potential for incomplete penetrance due to a late age of onset, unaffected individuals younger than 50 were excluded from the analysis. In this first analysis, early onset FCD in the two children was assumed to be caused by homozygosity for the mutation. Their parents were not known to be related, but it was possible the affected children were homozygous for the mutant allele because of distant consanguinity. Two copies of the dominant mutation might be expected to increase severity and to accelerate onset of the disease. We therefore modeled the pedigree as a recessive early-onset FCD trait, with an intermediate phenotype for the heterozygotes, which corresponded to late-onset disease. This was implemented in the linkage analysis program MLINK with the binary factors format.¹⁹ Using this model, we first obtained significant linkage to chromosome 13 with LOD scores of 3.08 at *D13S175* and 4.44 at *D13S1236*.

Revised Genetic Linkage Model

Analysis of the genotype data for familial relationships and the construction of haplotypes for chromosome 13^{18,20} confirmed that the fathers of each sibship (III-10 and III-16) were not consanguineous with their wives. This favored the alternative explanation that III-10 and III-16 had independently developed FCD, perhaps because of an unlinked mutation. In this second model, the affected children were assumed to have had early-onset FCD because they had inherited one dominant *FCD1* mutant allele from their mothers and a second, unmapped FCD gene from their fathers.

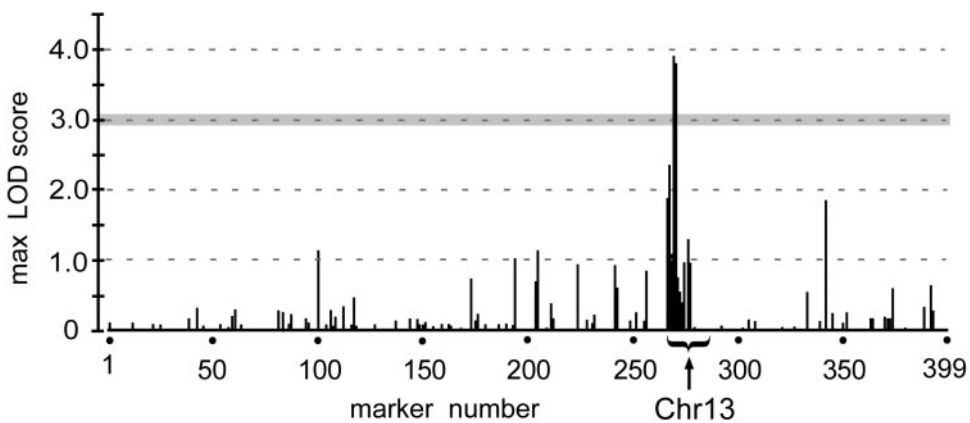
For purposes of linkage calculation, the two fathers (Fig. 1, sector symbols) were classified as unaffected because they did not carry the same *FCD1* mutation inherited by descendants of the founders, I-1 and I-2. Maximum LOD scores for each of the 399 markers (Fig. 3) revealed only one region with scores higher than 3.0. Scores for individual markers were calculated with MLINK using the same parameters described in Table 1, where linkage data is presented in more detail. As shown in Table 1, the first five markers of the chromosome 13 linkage group all gave maximum LOD scores at $\theta = 0$, indicating that crossovers between these markers and the disease locus were not detected. The $-\infty$ score at *D13S1304* indicated obligatory crossovers between *D13S1243* and *D13S1304*.

Finally, linkage analysis was also performed by treating the five-marker conserved haplotype as a single allele. Examination of the pedigree haplotypes (Fig. 4) yielded 13 different haplotypes. MLINK analysis with 13 alleles of equal frequency and complete penetrance gave a maximum LOD score of 4.05 at $\theta = 0$.

Genes in the Disease Interval

The linkage data (Table 1) and haplotype map (Fig. 4) formally place the disease interval between the P telomere and *D13S1304*. Although they constitute most of the interval, there is no assembled DNA sequence available for the centromere and the entire short (p) arm of chromosome 13. As one proceeds down the q arm of 13, the first genome assembly DNA sequence begins at 17.9 Mb from the p telomere, and the first known gene, *TUBA2*, is located at 18.65 Mb. Further down, there are a total of 44 known or predicted genes within the disease interval (Fig. 5). We have sequenced the exons of 10 of

FIGURE 3. Genome-wide genetic linkage of FCD. Maximum LOD scores were obtained for 399 polymorphic STR markers. Calculations used the same methods and fully penetrant dominant trait model described in Table 1. Scores are plotted as individual vertical bars, with 3.0 being the minimum necessary to establish linkage. Markers are ordered by chromosome, beginning with chromosome 1. Each chromosomal set follows the p-to-q order of the Marshfield linkage map. The horizontal bracket indicates all markers in the chromosome 13 linkage group.



these (Fig. 5, stars; see also Methods), but have not yet found FCD-associated mutations.

DISCUSSION

FCD1, the first locus for late-onset FCD, is defined as a 26.4-Mb interval extending from the 13p telomere to 13q12.13 (Fig. 5). One complication associated with this large interval is that the entire p arm of this acrocentric chromosome and the centromeric region have no sequence or clone contigs in the May 2004 assembly of the human genome sequence. Although assembled sequence is not available, 13p12 is known as the site of the *RNRI* nucleolus organizer (Online Mendelian Inheritance in Man [OMIM] 180450; <http://www.ncbi.nlm.nih.gov/Omim/> provided in the public domain by the National Center for Biotechnology Information, Bethesda, MD), which is composed of hundreds of tandem repeats of the 5s, 18s, and 28s ribosomal RNA genes.^{23,24} Otherwise, there are no known genes mapping to this interval, which contains large blocks of highly repetitive DNA. Another technical difficulty we have encountered is that no polymorphic genetic markers are available for this large, unknown region of chromosome 13. Therefore, although the family may exhibit crossover events that define an upper boundary for *FCD1* within 13p or 13q, we

cannot detect them. Although it seems unlikely that this interval contains candidate genes, we still cannot formally rule out that 13p contains functionally significant loci. There are a few genome database and literature references to protein-coding genes in 13p, and we have examined them in detail. However, all appear to be incorrect, and either are the result of typographical errors, or are in old publications reporting gene locations that have since been remapped elsewhere.

The portion of the *FCD1* interval that is represented in the sequenced genome assembly spans 13q12.11-q12.13 and covers 7.6 Mb. It includes 44 known and predicted protein-coding genes (Fig. 5). We have screened the exons of 10 of these (see Methods for details), but so far have found no variants beyond common polymorphisms. Of early interest were two closely related genes, *LOC387911* and *MGC48915*. Each of these has internal GXX collagen helix repeats and a C-terminal C1Q domain, features shared by other basal lamina collagens including *COL8A2*.^{7,8,15} Unfortunately, they contain no coding region mutations associated with FCD. These two candidate genes also do not appear to be major components of the cornea or Descemet's membrane. They are not represented in expressed sequence tag (EST) clones from cornea, or in SAGE libraries from the corneal endothelium.²⁵

Possible difficulties in identifying the *FCD1* mutation are its dominant nature and its mild, late-onset phenotype.²² The defect could be a noncoding region promoter mutation that causes a modest change in mRNA levels. Another possibility is that the *FCD1* mutation is a gene deletion that causes a phenotype through haploinsufficiency, which in turn causes a dominant mode of inheritance, with a potentially lethal homozygous phenotype. Unfortunately, conventional exon screening usually does not detect the deletion of a whole exon or gene. Testing this possibility will require an examination of the relative kinetics of PCR for each gene amplicon using quantitative PCR, or the observation of apparent non-Mendelian inheritance of polymorphisms within the gene. It may also be necessary to examine the disease chromosome for other large-scale rearrangements, such as inversions.^{22,26} Such chromosome breakage and nonhomologous reunion are known to cause dominant gain-of-function alleles by fusing coding sequences of a gene with novel promoter elements.

An intriguing feature of this particular pedigree is the finding that two parents with late-onset FCD can have a child with the early stages of classic FCD. This has yet to be reported elsewhere and was noted only during the course of a detailed examination of this particular family. Families with mutations in *COL8A2* show consistent early-onset of FCD, but it is a form of the disease with a very distinct clinical appearance and histopathologic abnormalities.^{8,14,15} In the two children we

TABLE 1. Genetic Linkage to 13pTel-13q12.13

Marker	Location (Mb)	Location (cM)	Lod Score		
			$\theta = 0$	Lod Max	θ Max
<i>D13S1316</i>	19.58	0.00	1.90	1.90	0.000
<i>D13S175</i>	19.75	6.03	2.38	2.38	0.000
<i>D13S250</i>	21.26	6.03	1.11	1.11	0.000
<i>D13S1236</i>	21.59	2.77	3.91	3.91	0.000
<i>D13S1243</i>	23.70	9.79	3.80	3.80	0.000
<i>D13S1304</i>	26.27	13.45	—	0.76	0.210
<i>D13S217</i>	28.27	17.21	−1.25	0.57	0.120
<i>D13S289</i>	30.16	21.51	0.41	0.41	0.000
<i>D13S171</i>	32.15	25.08	—	0.97	0.160

Detailed results of the analysis in Figure 3 are provided for the first seven markers of the Marshfield chromosome 13 linkage map. Markers are ordered by physical map position in megabases according to the May 2004 genome assembly. Recombination distance in centimorgans is from the Marshfield linkage map.²¹ Lod scores are calculated with the assumption of no recombination ($\theta = 0$), or the maximum lod score obtainable when recombination distance (θ) is varied. As in Figure 3, linkage was computed using MLINK, with the assumption of fully penetrant dominant inheritance, and individuals III-10 and III-16 (see Fig. 1) were scored as formally unaffected. This last feature of the linkage model reflects the observation that III-10 and III-16 are unrelated to III-11 and III-15 and that their FCD has an independent genetic basis.

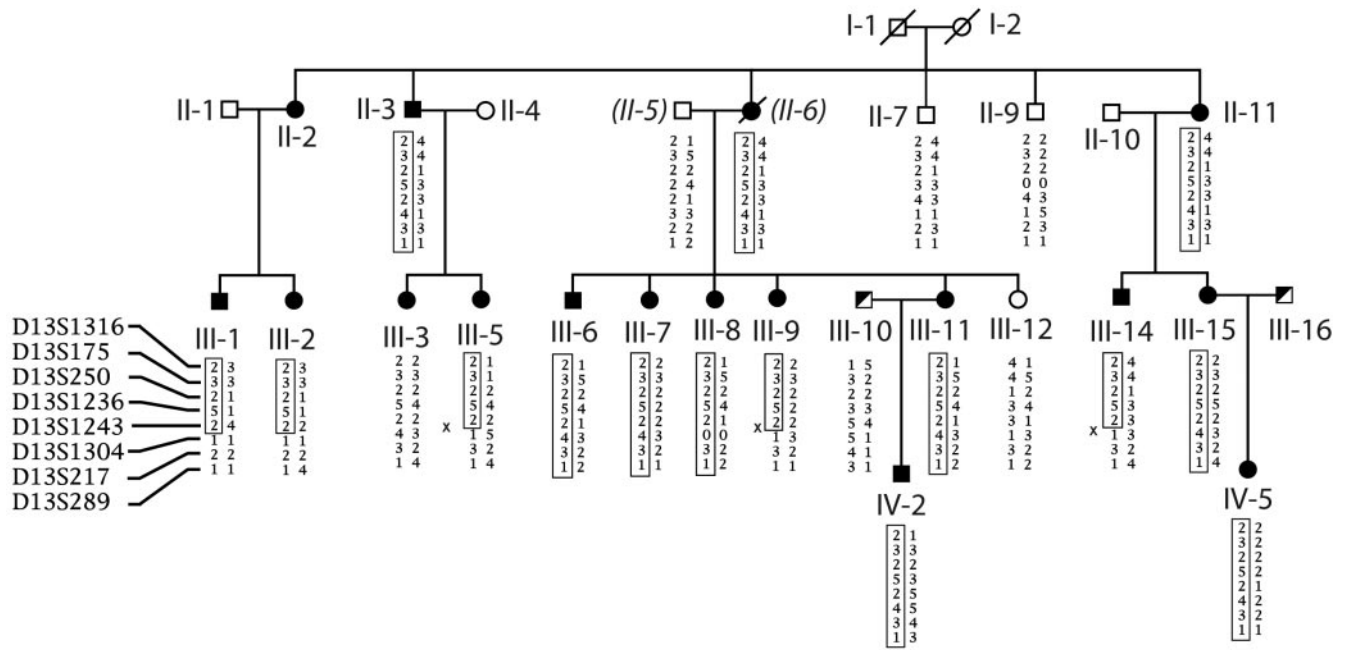


FIGURE 4. Haplotype analysis of the *FCD1* disease locus. Predicted haplotypes generated by Simwalk are displayed underneath individuals who were genotyped. The only exceptions are II-5 and II-6 (*italics*), for whom haplotypes were deduced from genotypes of their children. *Boxed numbers*: allele haplotypes found on disease-associated chromosomes. The *smaller box*, with markers *D13S1316* through *D13S1243*, contains a core haplotype common to all affected individuals descended from I-1 and I-2. *Sectored symbols*: FCD-affected individuals who are not descended from I-1 and I-2. Intervals where crossovers have occurred are indicated by an *x*.

report in this study, the guttae were indistinguishable from those described for conventional late-onset FCD.^{8,17} These findings open the possibility that the incidence of FCD in children is more frequent than previously thought. Another alternative is that that *FCD1* has a tendency toward earlier

onset and that this tendency is sensitive to unlinked genetic modifiers or environmental factors. In two instances, it is possible that digenic interaction with dominant FCD-causing mutations in other genes has accelerated onset of the disease by two to three decades.

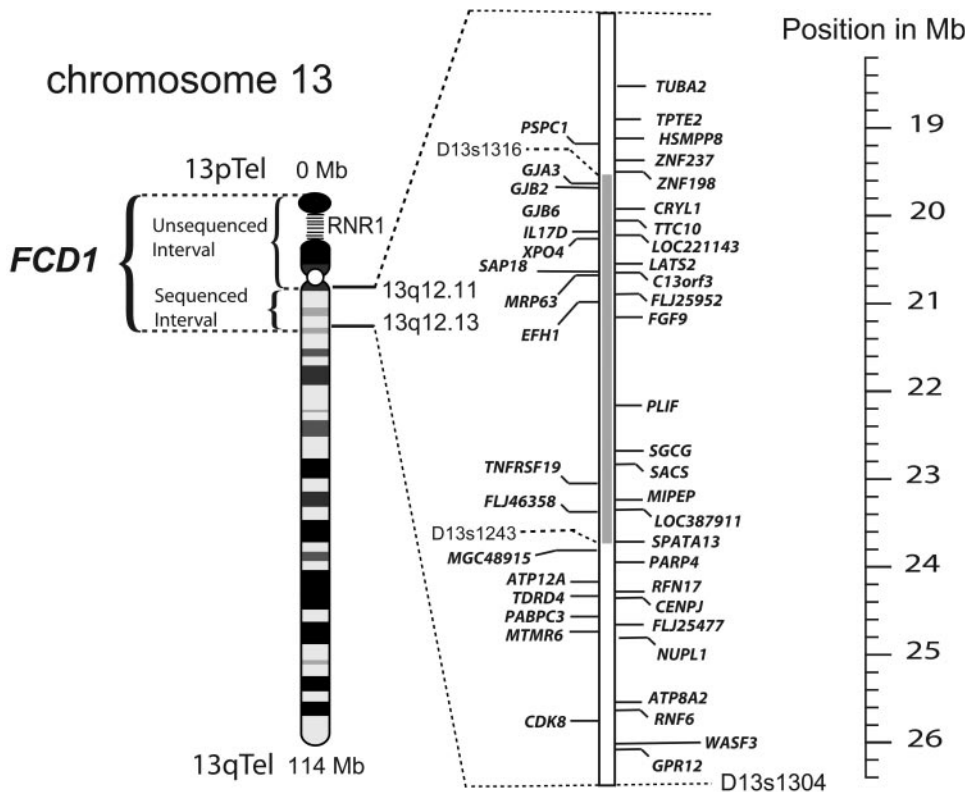


FIGURE 5. Genes in the *FCD1* disease interval. Ideogram of human chromosome 13, with *FCD1* interval indicated by vertical bracket. 13pTel, 13qTel indicate p and q telomeres, with nucleotide positions of 0 and ~114 million base pairs, respectively. *Right*: the 7.6-Mb FCD1 cytological interval, with genes mapped by nucleotide position (May 2004 human genome assembly). *Shaded area*: region within the disease locus, whereas 13pTel and *D13S1304* mark the outer boundaries of the interval. No protein coding genes are known to exist in the interval between *TUBA2* and 13pTel.

Acknowledgments

The authors thank Thomas A. Johnson for his assistance in facilitating the examination of the family and the use of his facilities, and Irene Maumenee of the Johns Hopkins Center for Hereditary Eye Diseases for identifying the proband of the pedigree.

References

1. Fuchs E. Dystrophia epithelialis corneae. *Graefes Arch Clin Exp Ophthalmol*. 1910;76:478-508.
2. Wilson SE, Bourne WM. Fuchs' dystrophy. *Cornea*. 1988;7:2-18.
3. Chang S W, Tuli S, Azar D. Corneal dystrophies. In: Traboulsi E, ed. *Genetic Diseases of the Eye: A Textbook and Atlas*. New York: Oxford University Press; 1998:217-266.
4. Klintworth GK. The molecular genetics of the corneal dystrophies: current status. *Front Biosci*. 2003;8:687-713.
5. Krachmer JH, Purcell JJ Jr, Young CW, Bucher KD. Corneal endothelial dystrophy. A study of 64 families. *Arch Ophthalmol*. 1978;96:2036-2039.
6. Marshall GE, Konstas AG, Lee WR. Immunogold fine structural localization of extracellular matrix components in aged human cornea. I. Types I-V collagen and laminin. *Graefes Arch Clin Exp Ophthalmol*. 1991;29:157-163.
7. Levy SG, Moss J, Sawda H, Dopping-Hepenstal PJC, McCartney ACE. The composition of wide-spaced collagen in normal and diseased Descemet's membrane. *Curr Eye Res*. 1996;15:45-52.
8. Gottsch JD, Sundin OH, Liu S, et al. Inheritance of a novel *COL8A2* mutation defines a distinct early-onset subtype of Fuchs corneal dystrophy. *Invest Ophthalmol Vis Sci*. 2005;46:1934-1939.
9. Waring GO, Bourne WM, Edelhauser HF, Kenyon KR. The corneal endothelium, normal and pathologic structure and function. *Ophthalmology*. 1982;89:531-590.
10. Bergmanson JP, Sheldon TM, Goosey JD. Fuchs' endothelial dystrophy: a fresh look at an aging disease. *Ophthalmic Physiol Opt*. 1999;19:210-222.
11. Thompson RW Jr, Price MO, Price FW Jr. Long-term graft survival after penetrating keratoplasty. *Ophthalmology*. 2003;110:1396-1402.
12. Cross HE, Maumenee AE, Cantolino SJ. Inheritance of Fuchs' endothelial dystrophy. *Arch Ophthalmol*. 1971;85:268-272.
13. Rosenblum, P, Stark WJ, Maumenee IH, Hirst LW, Maumenee AE. Hereditary Fuchs' dystrophy. *Am J Ophthalmol*. 1980;90:455-462.
14. Magovern M, Beauchamp B, McTigue JW, Baumiller RC. Inheritance of Fuchs' combined dystrophy. *Ophthalmology*. 1979;86:1897-1923.
15. Biswas S, Munier FL, Yardley J, et al. Missense mutations in *COL8A2*, the gene encoding the $\alpha 2$ chain of type VIII collagen, cause two forms of corneal endothelial dystrophy. *Hum Mol Genet*. 2001;10:2415-2423.
16. Kobayashi A, Fujiki K, Murakami A, et al. Analysis of *COL8A2* gene mutation in Japanese patients with Fuchs' endothelial dystrophy and posterior polymorphous dystrophy. *Jpn J Ophthalmol*. 2004;48:195-198.
17. Chiou AG, Kaufman SC, Beuerman RW, Ohta T, Soliman H, Kaufman HE. Confocal microscopy in cornea guttata and Fuchs' endothelial dystrophy. *Br J Ophthalmol*. 1999;83:185-189.
18. O'Connell JR, Weeks DE. PedCheck: A program for identification of genotype incompatibilities in linkage analysis. *Am J Hum Genet*. 1998;6:259-266.
19. Terwilliger JD, Ott J. *Handbook of Human Genetic Linkage*. Baltimore: Johns Hopkins University Press; 1994.
20. Sobel E, Lange K. Descent graphs in pedigree analysis: applications to haplotyping, location scores, and marker sharing statistics. *Am J Hum Genet*. 1996;58:1323-1337.
21. Broman KW, Murray JC, Sheffield VC, White RL, Weber JL. Comprehensive human genetic maps: individual and sex-specific variation in recombination. *Am J Hum Genet*. 1998;63:861-869.
22. Kazazian HH, Antonarakis SE. The varieties of mutation. *Prog Med Genet*. 1988;7:43-67.
23. Krystal M, D'Eustachio P, Ruddle FH, Arnheim N. Human nucleolus organizers on nonhomologous chromosomes can share the same ribosomal gene variants. *Proc Natl Acad Sci USA*. 1981;78:5744-5748.
24. Worton RG, Sutherland J, Sylvester JE, et al. Human ribosomal RNA genes: orientation of the tandem array and conservation of the 5-prime end. *Science*. 1988;239:64-68.
25. Gottsch JD, Bowers AL, Margulies EH, et al. Serial analysis of gene expression in the corneal endothelium of Fuchs' dystrophy. *Invest Ophthalmol Vis Sci*. 2003;44:594-599.
26. Mohammed FM, Krishna-Murthy DS, Farag TI, Al-Awadi SA, Al-Othman SA, Hammad I. Familial pericentric inversion of chromosome 13, 46,XX, inv (13)(p13;q11): a new variant. *Ann Genet*. 1993;36:181-185.